Chinese Journal of Natural Medicines

Natural diosmin alleviating obesity and nonalcoholic fatty liver disease by regulating the activating the AMP-activated protein kinase (AMPK) pathway

Can Liu, Siyu Hao, Mengdi Zhang, Xueyu Wang, Baiwang Chu, Tingjie Wen, Ruoyu Dang, Hua Sun

Citation: Can Liu, Siyu Hao, Mengdi Zhang, Xueyu Wang, Baiwang Chu, Tingjie Wen, Ruoyu Dang, Hua Sun, Natural diosmin alleviating obesity and nonalcoholic fatty liver disease by regulating the activating the AMP-activated protein kinase (AMPK) pathway, Chinese Journal of Natural Medicines, 2025, 23(7), 863-870. doi: 10.1016/S1875-5364(25)60914-9.

View online: https://doi.org/10.1016/S1875-5364(25)60914-9

Chinese Journal of Natural Medicines 23 (2025) 863-870

Contents lists available at ScienceDirect

Chinese Journal of Natural Medicines

journal homepage: www.cjnmcpu.com/

Original article

Natural diosmin alleviating obesity and nonalcoholic fatty liver disease by regulating the activating the AMP-activated protein kinase (AMPK) pathway

Can Liu[a,Δ], Siyu Hao[a,Δ], Mengdi Zhang[a], Xueyu Wang[a], Baiwang Chu[a], Tingjie Wen[a], Ruoyu Dang[b], Hua Sun[a,*]

[a] *College of Biotechnology, Tianjin University of Science & Technology, Tianjin 300457, China*
[b] *College of Pharmacy, Nankai University, Tianjin 300353, China*

ARTICLE INFO

Article history:
Received 16 June 2024
Revised 25 September 2024
Accepted 13 November 2024
Available online 20 July 2025

Keywords:
Diosmin
Lipometabolism
AMP-activated protein kinase
Obesity
Metabolic dysfunction-associated steatotic liver disease

ABSTRACT

Obesity and metabolic dysfunction-associated steatotic liver disease (MASLD) are linked to numerous chronic conditions, including cardiovascular disease, atherosclerosis, chronic kidney disease, and type II diabetes. Previous research identified the natural flavonoid diosmin, derived from *Chrysanthemum morifolium*, as a regulator of glucose metabolism. However, its effects on lipid metabolism and underlying mechanisms remained unexplored. The AMP-activated protein kinase (AMPK) pathway serves a critical function in glucose and lipid metabolism. The relationship between diosmin and the AMPK pathway has not been previously documented. This investigation examined diosmin's capacity to reduce lipid content through AMPK pathway activation in hepatoblastoma cell line G2 (HepG2) and 3T3-L1 cells. The study revealed that diosmin inhibits lipogenesis, indicating its potential as an anti-obesity agent in obese mice. Moreover, diosmin demonstrated effective MASLD alleviation *in vivo*. These findings suggest that diosmin may represent a promising therapeutic candidate for treating obesity and MASLD.

1. Introduction

Diosmin is a natural flavone glycoside derived from hesperidin, a flavanone predominantly present in citrus fruits. Diosmin occurs naturally in various plants, including *Galium verum*, and *Mentha canadensis* [1-3]. In clinical practice, diosmin primarily treats symptoms associated with venous and lymphatic insufficiency, including venous edema, thrombophlebitis, and deep vein thrombosis syndrome, as well as acute hemorrhoid symptoms [4,5]. Recent research has demonstrated that diosmin possesses a range of beneficial activities, including anti-inflammatory, anti-apoptotic, anti-tumor, and anti-diabetic properties [6-8]. Islam et al. demonstrated that diosmin shows promise as a therapeutic adjuvant against B[a]P-induced oxidative stress and lung damage [8]. Previous research by the authors revealed that diosmin, a natural flavonoid identified from *C. morifolium*, functions as a dual regulator of *α*-glucosidase and PTP-1B signaling pathways, indicating its potential application as a novel oral hypoglycemic drug or functional food ingredient [9]. However, diosmin's effects on lipid metabolism and its underlying mechanisms remain incompletely understood.

Metabolic dysfunction-associated steatotic liver disease (MASLD) represents the most prevalent chronic liver disease in western countries, emerging as a significant public health concern [10]. Research indicates that MASLD may become the leading indication for liver transplantation in future years [11]. MASLD correlates with various chronic conditions, including cardiovascular disease, atherosclerosis, chronic kidney disease, and type II diabetes [12-14]. The pathogenesis of MASLD is intrinsically linked to metabolic disorders, such as central obesity, dyslipidemia, hypertension, hyperglycemia, and persistent abnormal liver function [13-17]. Currently, no approved therapeutic interventions exist for MASLD, highlighting the critical need to identify effective pharmacological treatments.

AMP-activated protein kinase (AMPK), a serine/threonine protein kinase, functions as a cellular energy sensor [18]. Compromised cellular energy status increases the cellular AMP to ATP ratio, activating AMPK and promoting phosphorylation of its α subunit at Thr172 *via* upstream kinases. Since 1973, AMPK activity has been linked to HMG-CoA reductase (HMGCR) and acetyl-CoA carboxylase (ACC), key regulators of cholesterol and fatty acid synthesis [19-21]. AMPK serves as a critical master regulator of lipid metabolism, directly phosphorylating proteins or modulating gene transcription in specific tissues including liver, adipose, and muscle in mammals [22]. Research demonstrates that AMPK maintains human metabolic stability, including lipid and glucose metabolism [22-25]. Therefore, identifying drugs that regulate lipid metabolism through the AMPK pathway remains crucial for effective MASLD treatment [26-29]. The effects of diosmin on the AMPK pathway warrant further investigation [30].

This study demonstrates that diosmin reduced lipid content by activating the AMPK pathway in hepatoblastoma cell line G2 (HepG2) and 3T3-L1 cells. Furthermore, diosmin inhibited lipo-

* Corresponding author.
E-mail address: sunhua@tust.edu.cn
Δ These authors contributed equally to this work.

https://doi.org/10.1016/S1875-5364(25)60914-9

genesis, suggesting its potential as an anti-obesity agent in obese mice. Additionally, diosmin effectively alleviated MASLD *in vivo*. Collectively, these findings indicate that diosmin may be a promising candidate drug for the treatment of hyperlipidemia, obesity, and MASLD.

2. Materials and methods

2.1. Chemicals and reagents

Diosmin was obtained from Shanghai SAN Chemical Technology Co., Ltd. (Shanghai, China). HepG2 cells and 3T3-L1 preadipocytes mouse cell lines were procured from the Shanghai Institutes for Biological Sciences, Chinese Academy of Sciences (Shanghai, China). Dulbecco's modified Eagle's medium (DMEM) and penicillin-streptomycin were acquired from Mediatech (Herndon, VA, USA). Oil Red O, dexamethasone, and 3-isobutyl-1-methylxanthine (IBMX) were purchased from solution (Sigma)-Aldrich (St. Louis, MO, USA). Insulin was obtained from Novo Nordisk (Tianjin, China). Oleic acid, palmitic acid, linoleic acid, and arachidonic acid were acquired from Sigma, Inc. (St. Louis, MO, USA). Antibodies against AMPKα, phosphorylated (p)-AMPKα (Thr172), ACC, p-ACC (Ser79), and β-actin were obtained from Cell Signaling Technology (Beverly, MA, USA). Lovastatin was purchased from MERYER (Shanghai, China). 5-Amino-1-[(2*R*,3*R*,4*S*,5*R*)-3,4-dihydroxy-5-(hydroxymethyl)oxolan-2-yl]imidazole-4-carboxamide (AICAR) was acquired from Santa Cruz Biotechnology (Santa Cruz, CA, USA).

2.2. Induction of fatty liver cells using HepG2 cells

HepG2 cells were cultured in a DMEM complete medium, supplemented with 10% fetal bovine serum (FBS) and a 1% penicillin-streptomycin antibiotic solution. Cells were maintained in an atmosphere of 5% CO_2 at 37 °C. HepG2 cells at approximately 70% confluence were seeded at a density of 1×10^5 cells per well in a 6-well cell culture plate. After 24 h, the cells underwent serum starvation in a serum-free medium. Following a 12-h period of serum deprivation, the HepG2 cells were exposed to a mixture inducer solution containing 0.75 mmol·L^{-1} of oleic acid, palmitic acid, linoleic acid, and arachidonic acid to induce lipid accumulation. The cells were subsequently treated with varying concentrations of diosmin.

2.3. Mouse 3T3-L1 preadipocyte cell differentiation

The 3T3-L1 cells were cultured in DMEM, supplemented with 10% (*V*/*V*) newborn calf serum (NCS) and a 1% penicillin-streptomycin mixed solution as an antibiotic. The cells were maintained in an atmosphere of 5% CO_2 at 37 °C and grown to 80%–90% confluence. Subsequently, the 3T3-L1 cells were plated at a density of 1×10^6 cells per well. The cells were cultured for 2 d post-confluence, after which the primary medium was replaced with a medium containing 0.5 mmol·L^{-1} IBMX (storage density of 0.5 mol·L^{-1}), 1 μmol·L^{-1} DEX (storage density of 1 mmol·L^{-1}), and 10 μg·mL^{-1} insulin. After 2 d, the medium was exchanged with a medium containing 10 μg·mL^{-1} insulin and cultured with fetal calf serum medium for an additional 2 d. The differentiated cells were then prepared for subsequent experiments.

2.4. Cell viability assay

The cell viability assay was performed before the lipid accumulation experiment. HepG2 cells and 3T3-L1 preadipocytes were seeded into a 96-well plate. Diosmin was dissolved in dimethyl sulfoxide (DMSO) at various concentrations. The cells were incubated with different diosmin concentrations, with the DMSO-treated group serving as a control for cell viability detection using the methyl thiazolyl tetrazolium (MTT) assay (Sigma). The treated culture plates were then analyzed for cell viability using a Microplate Reader.

2.5. Oil red O staining

Prior to Oil red O staining, the cells were washed three times with phosphate-buffered saline (PBS). Oil red O was employed to stain intracellular lipids, as previously reported [31]. Specifically, the differentiated HepG2 and 3T3-L1 cells from the various groups were fixed with 4% polyformaldehyde for 30 min. The cells were washed three times with PBS, treated with 60% isopropanol for 5 min, and stained with Oil red O for 1 h in the dark at room temperature. Finally, the cells were washed with distilled water. The lipid droplets were dissolved in 100% isopropanol, and the absorbance was measured at 492 nm for quantification.

2.6. Nile red staining

The lipid content in HepG2 cells was evaluated through Nile red and 4',6-diamidino-2-phenylindole (DAPI) staining. A Nile Red stock solution (1 mg·mL^{-1}) was prepared in acetone, while a DAPI stock solution (10 mg·mL^{-1}) was maintained at −20 °C in dark conditions. HepG2 cells cultured in 6-well plates were incubated with Nile red at a final concentration of 10 μg·mL^{-1} and DAPI at a final concentration of 1 μg·mL^{-1} for 15 min at room temperature in darkness. Following the staining procedure, an inverted fluorescence microscope (Nikon, Melville, NY, United States) was employed to capture fluorescent images of the lipid content state.

2.7. Assay of triglyceride (TG) and total cholesterol (TC)

HepG2 and 3T3-L1 cells were seeded in 6-well plates at a density of 1×10^5 or 1×10^6 cells per well. Following incubation and differentiation induction, the HepG2 and 3T3-L1 cells received treatment with various concentrations of diosmin for the specified duration. The cells were subsequently washed three times with chilled PBS to remove glycerol. After centrifugation, the cells were collected and lysed with TG and TC lysate. The cells were maintained at room temperature for 10 min after mixing with the lysate. Protein quantification was performed on the cells. The collected cells underwent heating at 70 °C for 10 min, followed by centrifugation at 2000 r·min^{-1} for 5 min. The supernatant was utilized for enzymatic determination. TG and TC concentrations were measured using an enzymatic kit (Applygen Technologies Inc, Beijing, China).

2.8. Western blotting analysis

HepG2 cells at 1×10^5 per well or 3T3-L1 cells at a density of 1×10^6 cells/well were plated in 60 mm culture dishes. The cells underwent separate differentiation induction and diosmin treatment. After experiment completion, the cells were digested with trypsin and collected. The cells underwent three washes with chilled PBS and centrifugation at 2500 r·min^{-1} for 5 min. Following protein lysate addition, the cells were lysed on ice for 60 min, then centrifuged at 13 500 r·min^{-1} at 4 °C for 20 min. Protein content was determined using a bicinchoninic acid assay (BCA) protein assay kit. Equal protein solution amounts were electrophoresed on sodium dodecyl sulfate-polyacrylamide gels (SDS-PAGE) and transferred onto a polyvinylidene fluoride (PVDF) membrane. The membrane transfer proceeded for 2 h, followed by membrane blocking with 5% non-fat milk in 1 × PBS containing 0.5% Tween 20 (PBST) for 1 h at room temperature. The blots were incubated overnight at 4 °C with anti-p-AMPK, anti-AMPK, anti-p-ACC, anti-ACC, and anti-β-actin, followed by incubation with anti-mouse antibody and anti-rabbit antibody (1∶5000 dilu-

tion) for 2 h at room temperature. Pierce™ ECL Western blotting substrate (Thermo Scientific, Waltham, MA) was used to detect the bands [32].

2.9. Animal and diets

Forty-nine male C57BL/6J mice were acquired from Beijing Weitong Lihua Laboratory Animal Technology Co., Ltd. (Beijing, China). This animal study was approved by the Academic Committee of Tianjin University of Science and Technology and conducted in accordance with all applicable animal welfare regulations (LLSC20250501).

The study comprised 7 mice fed a low-fat diet (TP23302) supplied by Nantong Troffei Feed Technology Co., Ltd. (Nantong, China) as the normal group. The remaining 42 mice received a high-fat diet (TP23300, 60% fat content) to establish an obesity model and serve as the drug administration group. All mice underwent continuous feeding for 27 d.

2.10. Animal experiments

Following a 12-d high-fat diet administration, mice in the model group exhibited a 20% increase in body weight compared to the normal group, confirming successful establishment of the obesity model. Subsequently, diosmin was administered daily *via* gavage for 15 d. The mice were allocated into three groups, receiving diosmin doses of 400, 150, and 50 mg·kg^{-1}, respectively. The positive control group received 150 mg·kg^{-1} AICAR and 400 mg·kg^{-1} L-carnitine *via* gavage. After 15 d, the liver, kidney, white adipose tissue, and other tissues were immediately dissected, washed, and weighed. A portion of liver and white fat tissue was preserved in 4% paraformaldehyde fixative for subsequent staining. The remaining liver and adipose tissue were flash-frozen in liquid nitrogen and stored at −80 °C for future analysis.

2.11. Statistical analysis

The data are expressed as mean ± standard deviation (SD). Statistical evaluation was performed using one-way analysis of variance (ANOVA) or two-tailed independent Student's *t*-tests with Prism 5.0 software (GraphPad Software, La Jolla, CA, USA). A *P*-value below 0.05 was deemed statistically significant compared to the Model group.

3. Results and discussion

3.1. Diosmin induces a lipid decrease in HepG2 cells

This investigation evaluated the cytotoxicity of diosmin in HepG2 cells. HepG2 cells were exposed to various concentrations of diosmin and 10 μmol·L^{-1} lovastatin. As illustrated in Fig. 1A, no significant cytotoxicity was observed across treatment groups. These concentrations were subsequently utilized in further experiments. To examine diosmin's effect on HepG2 cells, intracellular lipid droplets underwent Oil red O staining, followed by lipid content quantification. Diosmin reduced lipid droplet accumulation in a dose-dependent manner. Treatment with 10, 30, and 80 μmol·L^{-1} of diosmin and 10 μmol·L^{-1} lovastatin decreased total lipid content in HepG2 cells by 28.98%, 64.65%, and 89.59%, re-

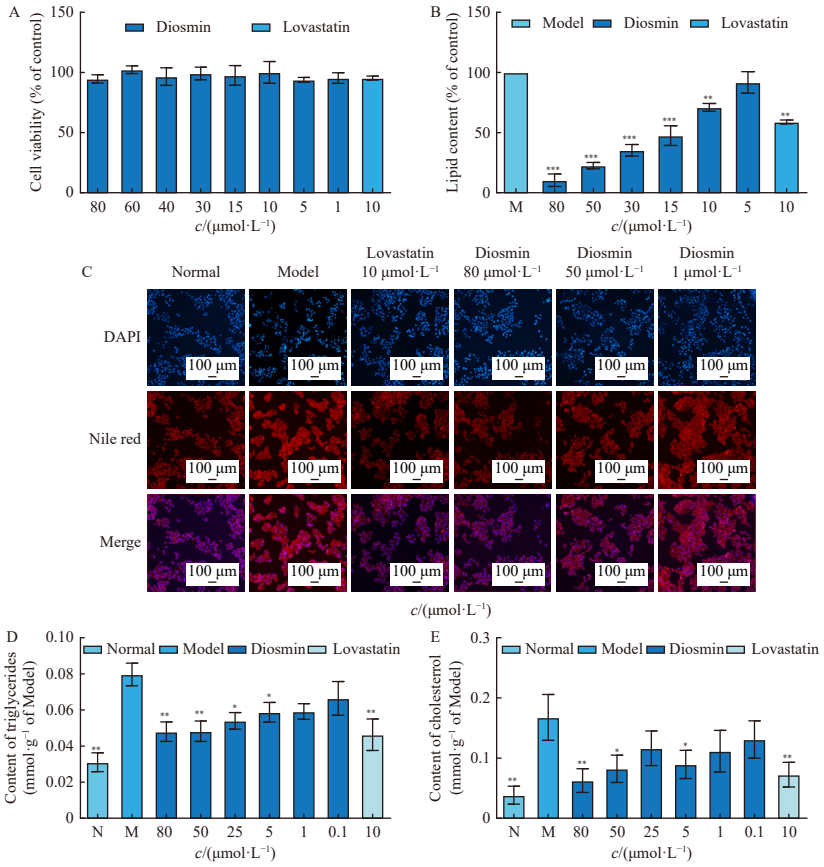

Fig. 1 The lipid-decreasing effect of diosmin in HepG2 cells. (A) The effect of diosmin and lovastatin on cytotoxicity. HepG2 cells were treated with different concentrations of diosmin and 10 μmol·L^{-1} lovastatin for 24 h, and cell viability was measured by MTT assay. (B) The cells were stained with Oil red O, and lipid content was quantified. (C) The cells were fixed with polyformaldehyde and stained with Nile red and DAPI. (D) The intracellular TG and cholesterol content were determined by analysis of TG and total cholesterol (TC) kits, respectively. (E) The intracellular cholesterol content was determined by analysis of TC kits. The "Normal" condition refers to cells not cultured in the induced differentiation medium and without diosmin treatment. The "Model" condition refers to cells cultured in the induced differentiation medium without diosmin treatment. Data are represented as means ± SD (n = 3). $^{*}P < 0.05$, $^{**}P < 0.01$, and $^{***}P < 0.001$ *vs* the Model group.

spectively, while 10 μmol·L^{-1} lovastatin reduced lipid content by 41.31% (Fig. 1B). Similarly, Nile red and DAPI staining revealed dose-dependent hypolipidemic effects of diosmin (Fig. 1C). Additionally, TG and cholesterol accumulation decreased when cells were incubated with different diosmin concentrations and 10 μmol·L^{-1} lovastatin (Figs. 1D and 1E). These findings demonstrate diosmin's lipid-lowering effects in HepG2 cells.

3.2. Diosmin induces lipid decreases in 3T3-L1 preadipocytes and mature 3T3-L1 adipocytes

This investigation evaluated the cytotoxicity of diosmin and lovastatin in 3T3-L1 preadipocytes and mature 3T3-L1 adipocytes. The cells underwent treatment with various concentrations of diosmin and 10 μmol·L^{-1} lovastatin. As illustrated in Figs. 2A and 2C, the tested concentrations exhibited no significant toxicity and were utilized in subsequent experiments. To examine diosmin's effect on 3T3-L1 preadipocytes, intracellular lipid droplets underwent Oil red O staining, followed by lipid content quantification. Diosmin demonstrated dose-dependent reduction in lipid droplet accumulation. The total lipid content in cells treated with 10, 15, and 40 μmol·L^{-1} of diosmin decreased to 54.19%, 68.53%, and 84.25%, respectively (Fig. 2B). The research also analyzed diosmin's effect on mature 3T3-L1 adipocytes. The total lipid content in cells treated with 10, 50, and 100 μmol·L^{-1} of diosmin decreased to 36.15%, 69.07%, and 77.05%, respectively (Fig. 2D). Additionally, TG and cholesterol accumulation in mature 3T3-L1 adipocytes decreased significantly when cells were incubated with different diosmin concentrations and 10 μmol·L^{-1} lovastatin (Figs. 2E and 2F). These findings demonstrate diosmin's lipid-decreasing effects in both 3T3-L1 preadipocytes and mature 3T3-L1 adipocytes.

3.3. Diosmin modulates lipid metabolism by regulating the AMPK pathway in cells

Extensive research indicates that AMPK functions as a critical regulator of cellular energy homeostasis, with a significant role in lipid metabolism. AMPK promotes fatty acid oxidation through ACC inhibition, thereby reducing malonyl-CoA and fatty acid production. This mechanism has shown effectiveness in lipid reduction [33-35]. Consequently, this study investigated whether diosmin regulates the AMPK pathway in cells. Initially, diosmin's effect on the AMPK pathway was examined in HepG2 cells. As demonstrated in Figs. 3A–3C, diosmin treatment enhanced AMPK and ACC phosphorylation in a dose-dependent manner, aligning with the effects of the AMPK activator, AICAR. This hypothesis was further validated in 3T3-L1 preadipocytes and mature 3T3-L1 adipocytes. The results paralleled those observed in HepG2 cells, where diosmin incubation significantly enhanced AMPK and ACC phosphorylation (Figs. 3D–3I). These results indicate that diosmin exhibits lipid-lowering effects through AMPK pathway regulation in HepG2, 3T3-L1 preadipocytes, and mature 3T3-L1 adipocytes.

3.4. Diosmin affects lipid metabolism in obese mice

The lipid-reducing effects of diosmin were investigated through the establishment of obese mouse models using a high-fat diet protocol over 12 d. Following model establishment, the mice were randomly assigned to groups and received diosmin administration for 15 d. Initial assessments focused on diosmin's influence on food and water consumption in obese mice. The findings demonstrated that diosmin administration led to a significant reduction in both average food and water intake (Figs. 4A and 4B). Analysis of organ indices revealed significant reductions in liver, kidney, and spleen weights in diosmin-treated obese mice compared to the Model group. The liver, kidney, and spleen indices exhibited marked decreases (Fig. 4C). These observations indicate that diosmin effectively attenuated obesity-induced organ enlargement.

Assessment of adipose tissue provides a critical indicator for anti-obesity efficacy. White adipose tissue, recognized as a primary contributor to obesity, presents substantial health risks. The regulation of white lipogenesis offers a promising therapeutic approach for obesity treatment. This investigation involved the examination, weight measurement, and photographic documentation of epididymal white adipose tissue, perirenal white adipose tissue, intestinal mucosal white adipose tissue, and scapular brown adipose tissue in mice. The results demonstrated that diosmin treatment significantly decreased the mass of epididymal white adipose tissue, perirenal white adipose tissue, intestinal mucosal white adipose tissue, and brown adipose tissue (Figs. 4D–4F). These findings indicate that diosmin exhibits anti-obesity properties through the inhibition of lipogenesis.

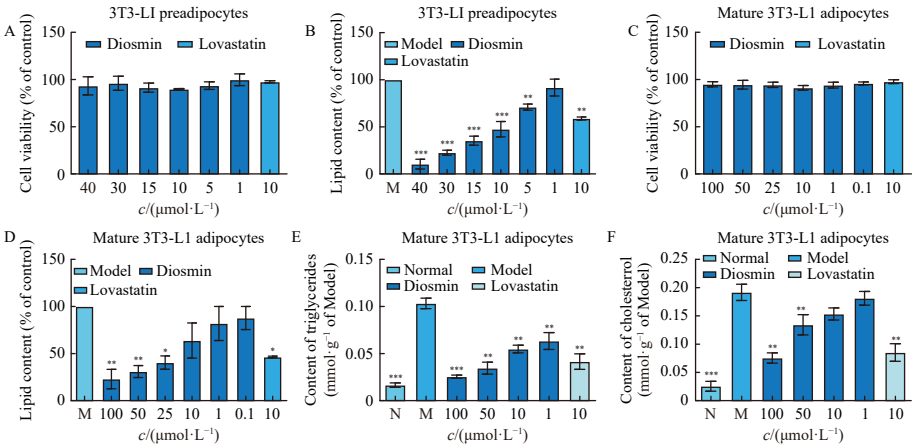

Fig. 2 The lipid-decreasing effect of diosmin in 3T3-L1 preadipocytes, and mature 3T3-L1 adipocytes. (A) The cytotoxicity effect of diosmin and lovastatin was assessed. 3T3-L1 preadipocytes were treated with varying concentrations of diosmin and 10 μmol·L^{-1} lovastatin for 24 h, and cell viability was measured using the MTT assay. (B) 3T3-L1 preadipocytes were stained with Oil red O, and the lipid content was quantified. (C) The cytotoxicity effect of diosmin and lovastatin was assessed. Mature 3T3-L1 adipocytes were treated with varying concentrations of diosmin and 10 μmol·L^{-1} lovastatin for 24 h, and cell viability was measured using the MTT assay. (D) Mature 3T3-L1 adipocytes were stained with Oil red O, and the lipid content was quantified. (E and F) The intracellular TG and cholesterol content were determined using TG and TC analysis kits, respectively. The "Normal" group represents cells not cultured in an induced differentiation medium or treated with diosmin, while the "Model" group represents cells cultured in an induced differentiation medium without diosmin treatment. Data are presented as means ± SD (n = 3). $^{*}P < 0.05$, $^{**}P < 0.01$, and $^{***}P < 0.001$ *vs* the Model group.

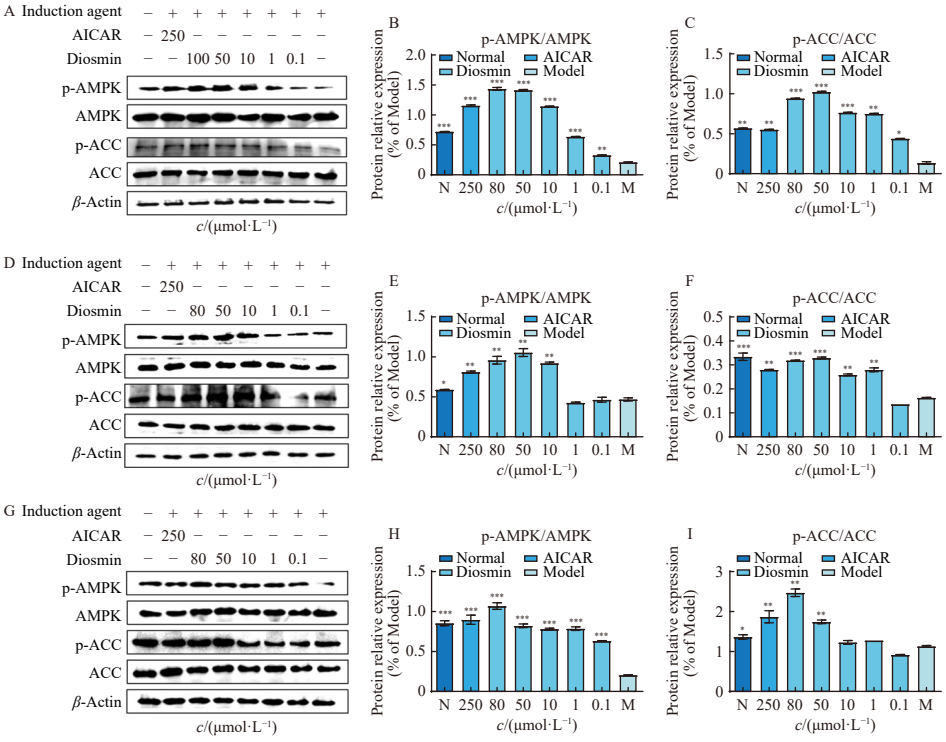

Fig. 3 Diosmin regulates the AMPK pathway in HepG2 cells, 3T3-L1 preadipocytes and mature 3T3-L1 adipocytes. (A) Immunoblot analysis of HepG2 cells reveals the expression of AMPK, p-AMPK, ACC, p-ACC, and *β*-actin. (B) Statistical quantification of the relative p-AMPK/AMPK protein levels in HepG2 cells. (C) Statistical analysis of the relative p-ACC/ACC protein levels in HepG2 cells. (D) Immunoblots of 3T3-L1 preadipocytes for AMPK, p-AMPK, ACC, p-ACC, and *β*-actin. (E) Statistical analysis of the relative p-AMPK/AMPK protein levels in 3T3-L1 preadipocytes. (F) Statistical analysis of the relative p-ACC/ACC protein levels in 3T3-L1 preadipocytes. (G) Immunoblots of mature 3T3-L1 adipocytes for AMPK, p-AMPK, ACC, p-ACC, and *β*-actin. (H) Statistical quantification of the relative p-AMPK/AMPK protein levels in mature 3T3-L1 adipocytes. (I) Statistical analysis of the relative p-ACC/ACC protein levels in mature 3T3-L1 adipocytes. The "Normal" condition represents cells cultured in the absence of diosmin treatment, while the "Model" condition denotes cells cultured in a differentiation medium with induction agents but without diosmin treatment. Data are presented as means ± SEM (n = 3). $^{*}P < 0.05$, $^{**}P < 0.01$, and $^{***}P < 0.001$ *vs* the Model group.

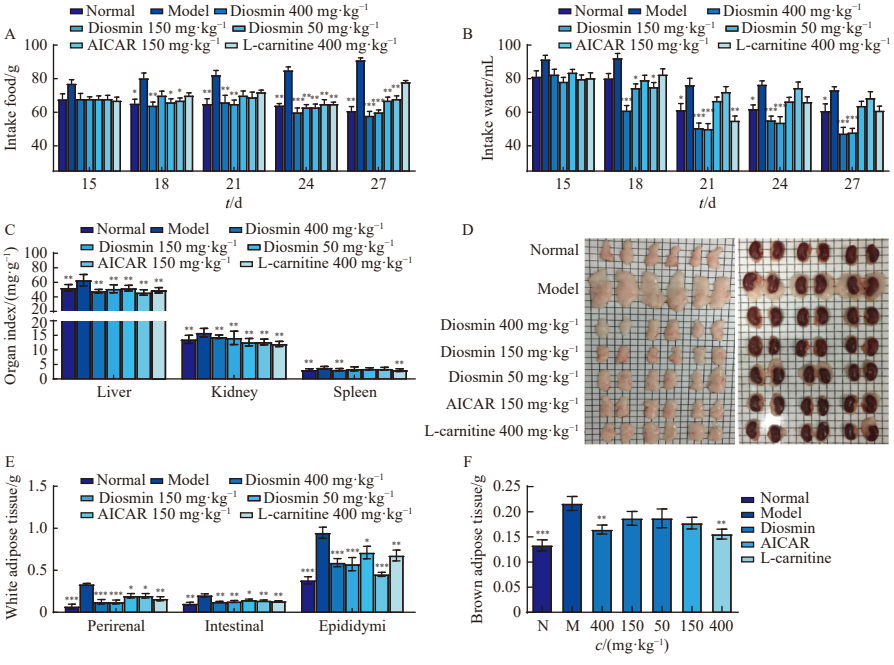

Fig. 4 Diosmin affects lipid metabolism in obese mice. (A) The average food intake of obese mice treated with diosmin is shown. (B) The average water intake of obese mice treated with diosmin is presented. (C) The organ indexes of the liver, kidney, and spleen are depicted. (D) The morphological effect of diosmin on epididymal and perirenal white adipose tissue is displayed. (E) Diosmin inhibited white lipogenesis in epididymal, perirenal, and intestinal white adipose tissue. (F) The effect of diosmin on the weight of brown adipose tissue is reported. Data are represented as means ± SEM (n = 7). $^{*}P < 0.05$, $^{**}P < 0.01$, and $^{***}P < 0.001$ *vs* the Model group.

3.5. Diosmin improves serum indices in MASLD mice

MASLD represents a significant risk factor for hepatocellular carcinoma. Abnormal lipid metabolism demonstrates a strong correlation with MASLD progression [36, 37]. To investigate diosmin's effects on MASLD, this study established a MASLD mouse model and evaluated serum parameters. As illustrated in Figs. 5A–5F, pitavastatin (which demonstrates beneficial and safe ef-

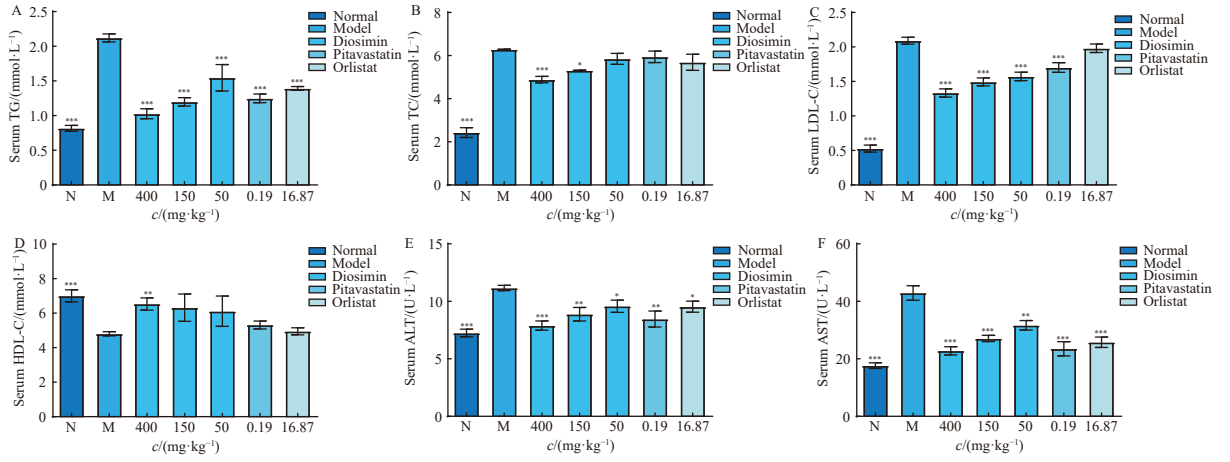

Fig. 5 Diosmin ameliorates the serum indices in MASLD mice. The serum levels of TG (A), TC (B), LDL-C (C), HDL-C (D), ALT (E), and AST (F) were evaluated. Data are represented as mean ± SEM (n = 6). $^{*}P < 0.05$, $^{**}P < 0.01$, and $^{***}P < 0.001$ *vs* the Model group.

fects in MASLD/MASH patients) [38], and orlistat (an anti-obesity drug showing beneficial effects on hepatic steatosis and inflammation) [39, 40] served as positive controls. The levels of TG, TC, low-density lipoprotein-cholesterol (LDL-C), alanine transaminase (ALT), and aspartate transaminase (AST) increased significantly, while high-density lipoprotein-cholesterol (HDL-C) decreased significantly in the tyloxapol-induced MASLD mouse model. These findings indicated hyperlipidemia, and elevated serum levels of ALT and AST suggested hepatocyte injury, inflammation, and hepatic fibrosis [25]. Diosmin reduced the serum levels of TC, TG, LDL-C, HDL-C, ALT, and AST in a dose-dependent manner in MASLD mice. These results demonstrate that diosmin effectively normalized serum parameters in the MASLD mouse model.

3.6. Diosmin ameliorates white adipogenesis, hepatic steatosis, and biomarkers in MASLD mice

To further examine the lipid-decreasing effects of diosmin in MASLD mice, researchers analyzed the epididymal white adipose tissue, perirenal white adipose tissue, and intestinal mucosal white adipose tissue through dissection, weighing, and photography. The results demonstrate that diosmin significantly reduced lipogenesis in these tissue types (Figs. 6A and 6B). These findings indicate that diosmin inhibited lipogenesis in the MASLD mouse model.

This investigation examined changes in liver morphology and biochemical indicators in a MASLD mouse model and the effects of diosmin treatment. Liver samples underwent dissection and various staining procedures to evaluate impacts on lipid accumulation and liver tissue structure. The results revealed that the tyloxapol-induced MASLD model group exhibited hepatomegaly, which diosmin treatment partially ameliorated (Fig. 6C). Oil red O staining demonstrated that diosmin significantly reduced lipid droplets and fat vacuoles in liver tissue sections (Fig. 6D). Similarly, diosmin, orlistat, and pitavastatin administration decreased lipid levels and areas stained with Masson's trichrome, enhancing the appearance of hepatic lobules (Fig. 6E). Further analysis of diosmin's effect on liver function in MASLD mice revealed significantly elevated levels of TG, TC, LDL-C, ALT, and AST in the MASLD model, while HDL-C decreased. Diosmin effectively modulated these biochemical indicators (Figs. 6F–6K). Moreover, diosmin enhanced the hepatic oxidative stress response, increasing SOD levels while reducing malondialdehyde (MDA) levels (Figs. 6L and 6N). The compound also suppressed the hepatic inflammatory response, as indicated by decreased levels of the pro-inflammatory cytokine, interleukin-6 (IL-6) (Fig. 6M). These findings demonstrate that diosmin effectively inhibited hepatic steatosis and normalized liver indices in the MASLD mouse model, suggesting its potential therapeutic value in MASLD management.

4. Conclusions

Diosmin, a flavanone predominantly found in citrus fruits [41], is primarily prescribed for treating symptoms associated with

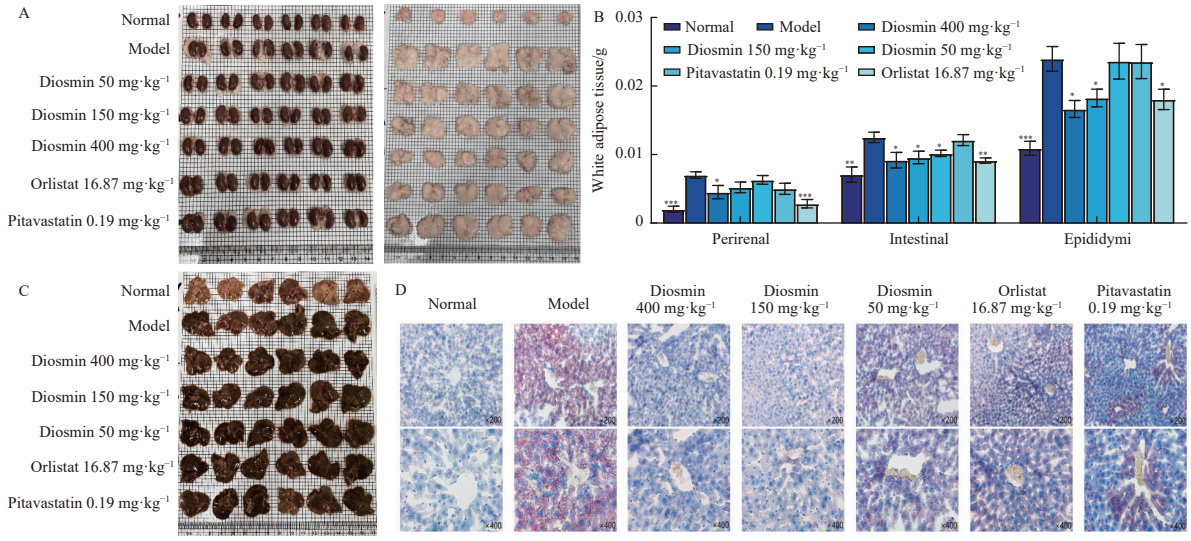

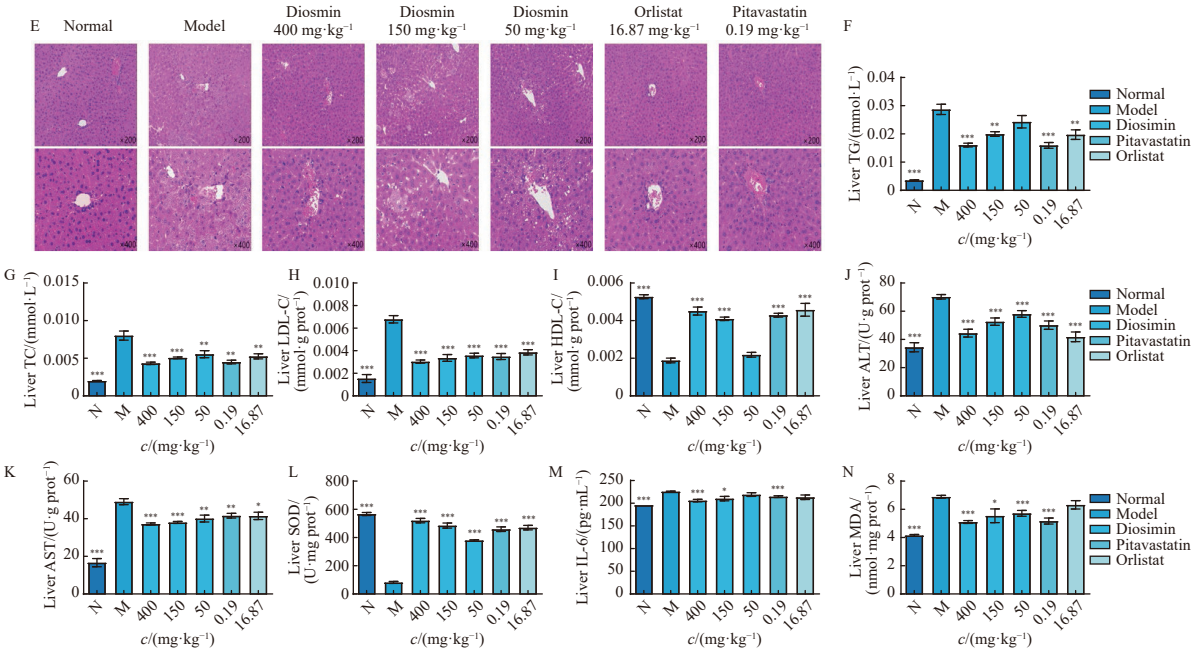

Fig. 6 Diosmin ameliorates white lipogenesis, liver steatosis and indices in MASLD mice. (A) The physical appearance of epididymal and perirenal white adipose tissue is presented. (B) Diosmin inhibited white lipogenesis in epididymal, perirenal, and intestinal white adipose tissue. (C) The appearance of the liver is shown. (D) Oil red O staining of the liver is depicted. (E) Masson's trichrome staining of the liver is provided. The liver levels of TG (F), TC (G), LDL-C (H), HDL-C (I), ALT (J), AST (K), SOD (L), Interleukin-6 (IL-6) (M), and MDA (N) are presented. Data are represented as mean ± SEM (n = 6). $^{*}P < 0.05$, $^{**}P < 0.01$, $^{***}P < 0.001$ *vs* the Model group.

venous and lymphatic insufficiency, including venous edema, thrombophlebitis, and deep vein thrombosis syndrome, as well as the management of acute hemorrhoids. Recent research indicates that diosmin demonstrates anti-inflammatory, anti-apoptotic, anti-tumor, and anti-diabetic properties, highlighting its potential for broader clinical applications.

Diosmin, a phytochemical compound, effectively reduced intracellular lipid content, TG and TC levels in HepG2 cells, 3T3-L1 preadipocytes, and mature 3T3-L1 adipocytes. This reduction occurred through activation of the AMPK pathway and subsequent phosphorylation of the downstream protein ACC [42]. The AMPK-mediated energy switch regulates cell growth and various cellular processes, including lipid and glucose metabolism. Additionally, diosmin exhibited positive effects on food intake, water intake, and organ enlargement in obese animal models, demonstrating its anti-obesity properties. In a MASLD mouse model, diosmin effectively restored the serum levels of TG, TC, LDL-C, HDL-C, ALT, and AST, while also regulating white lipogenesis, liver steatosis, and liver indices of TG, TC, LDL-C, HDL-C, ALT, and AST after tyloxapol-induction.

In conclusion, these findings indicate that diosmin may effectively regulate energy metabolism, normalize lipid metabolism disorders, and enhance therapeutic outcomes in hyperlipidemia, obesity, and MASLD.

Funding

This work was supported by the Innovation and Entrepreneurship Team Project of Jiangsu Province (No. JSSCTD202133).

Declaration of competing interest

These authors have no conflict of interest to declare.

References

1 Benavente-Garcia O, Castillo J. Update on uses and properties of citrus flavonoids: new findings in anticancer, cardiovascular, and anti-inflammatory activity. *J Agric Food Chem*. 2008;56(15):6185-6205. https://doi.org/10.1021/jf8006568.

2 Inoue T, Sugimoto Y, Masuda H, et al. Antiallergic effect of flavonoid glycosides obtained from *Mentha piperita* L. *Biol Pharm Bull*. 2002;25(2):256-259. https://doi.org/10.1248/bpb.25.256.

3 Cheng C, Zhang H, Li Y, et al. The effect of diosmin on the blood proteome in a rat model of venous thrombosis. *Int J Biol Macromol*. 2017;104(Pt A):778-787. https://doi.org/10.1016/j.ijbiomac.2017.06.045.

4 Giannini I, Amato A, Basso L, et al. Flavonoids mixture (diosmin, troxerutin, hesperidin) in the treatment of acute hemorrhoidal disease: a prospective, randomized, triple-blind, controlled trial. *Tech Coloproctol*. 2015;19(6):339-345. https://doi.org/10.1007/s10151-015-1302-9.

5 Bush R, Comerota A, Meissner M, et al. Recommendations for the medical management of chronic venous disease: the role of micronized purified flavanoid fraction (MPFF). *Phlebology*. 2017;32(1_suppl):3-19. https://doi.org/10.1177/0268355517692221.

6 Shalkami AS, Hassan M, Bakr AG. Anti-inflammatory, antioxidant and anti-apoptotic activity of diosmin in acetic acid-induced ulcerative colitis. *Hum Exp Toxicol*. 2018;37(1):78-86. https://doi.org/10.1177/0960327117694075.

7 Gopalakrishnan V, Iyyam PS, Subramanian SP. Synthesis, spectral characterization, and biochemical evaluation of antidiabetic properties of a new zinc-diosmin complex studied in high fat diet fed-low dose streptozotocin induced experimental type 2 diabetes in rats. *Biochem Res Int*. 2015;2015:350829. https://doi.org/10.1155/2015/350829.

8 Islam J, Shree A, Afzal SM, et al. Protective effect of diosmin against benzo(a) pyrene-induced lung injury in Swiss albino mice. *Environ Toxicol*. 2020;35(7):747-757. https://doi.org/10.1002/tox.22909.

9 Chen M, Wang K, Zhang Y, et al. New insights into the biological activities of *Chrysanthemum morifolium*: natural flavonoids alleviate diabetes by targeting α-glucosidase and the PTP-1B signaling pathway. *Eur J Med Chem*. 2019;178:108-115. https://doi.org/10.1016/j.ejmech.2019.05.083.

10 Younossi Z, Anstee QM, Marietti M, et al. Global burden of NAFLD and NASH: trends, predictions, risk factors and prevention. *Nat Rev Gastroenterol Hepatol*. 2018;15(1):11-20. https://doi.org/10.1038/nrgastro.2017.109.

11 Byrne CD, Targher G. NAFLD: a multisystem disease. *J Hepatol*. 2015;52(1 Suppl):S47-64. https://doi.org/10.1016/j.jhep.2014.12.012.

12 Després JP, Lemieux I, Bergeron J, et al. Abdominal obesity and the metabolic syndrome: contribution to global cardiometabolic risk. *Arterioscler Thromb Vasc Biol*. 2008;28(6):1039-1049. https://doi.org/10.1161/ATVBAHA.107.159228.

13 Pouwels S, Sakran N, Graham Y, et al. Non-alcoholic fatty liver disease (NAFLD): a review of pathophysiology, clinical management and effects of weight loss. *BMC Endocr Disord*. 2022;22(1):63. https://doi.org/10.1186/s12902-022-00980-1.

14 Guo X, Yin X, Liu Z, et al. Non-alcoholic fatty liver disease (NAFLD) pathogenesis and natural products for prevention and treatment. *Int J Mol Sci*. 2022;23(24):15489. https://doi.org/10.3390/ijms232415489.

15 Alqahtani SA, Schattenberg JM. NAFLD in the elderly. *Clin Interv Aging*. 2021;16:1633-1649. https://doi.org/10.2147/CIA.S295524.

16 Rong L, Zou J, Ran W, et al. Advancements in the treatment of non-alcoholic fatty liver disease (NAFLD). *Front Endocrinol (Lausanne)*. 2023;13:1087260. https://doi.org/10.3389/fendo.2022.1087260.

17 Xu R, Pan J, Zhou W, et al. Recent advances in lean NAFLD. *Biomed Pharmacother*. 2022;153:113331. https://doi.org/10.1016/j.biopha.2022.113331.

18 Grahame HD. Regulation of AMP-activated protein kinase by natural and synthetic activators. *Acta Pharm Sin B*. 2016;6(1):1-19. https://doi.org/10.1016/j.apsb.2015.06.002.

19 Beg ZH, Allmann DW, Gibson DM. Modulation of 3-hydroxy-3-methylglutaryl coenzyme A reductase activity with cAMP and with protein fractions of rat liver cytosol. *Biochem Bioph Res Commun*. 1973;54(4):1362-1369. https://doi.org/10.1016/0006-291X(73)91137-6.

20 Novikova DS, Garabadzhiu AV, Melino G, et al. AMP-activated protein kinase: structure, function, and role in pathological processes. *Biochemistry (Moscow)*. 2015;80(2):127-144. https://doi.org/10.1134/S0006297915020017.

21 Carlson CA, Kim KH. Regulation of hepatic acetyl coenzyme A carboxylase by phosphorylation and dephosphorylation. *J Biol Chem*. 1973;248(1):378-380. https://doi.org/10.1016/S0021-9258(19)44486-4.

22 Wang Q, Liu S, Zhai A, et al. AMPK-mediated regulation of lipid metabolism by phosphorylation. *Biol Pharm Bull*. 2018;41(7):985-993. https://doi.org/10.1248/bpb.b17-00724.

23 Huang R, Guo F, Li Y, et al. Activation of AMPK by triptolide alleviates nonalcoholic fatty liver disease by improving hepatic lipid metabolism, inflammation and fibrosis. *Phytomedicine*. 2021;92:153739. https://doi.org/10.1016/j.phymed.2021.153739.

24 Gao L, Xu Z, Huang Z, et al. CPI-613 rewires lipid metabolism to enhance pancreatic cancer apoptosis *via* the AMPK-ACC signaling. *J Exp Clin Cancer Res*. 2020;39(1):73. https://doi.org/10.1186/s13046-020-01579-x.

25 Zhang M, Wang Z, Hao S, et al. Synthesis of natural 3'-prenylchalconaringenin and biological evaluation of ameliorating non-alcoholic fatty liver disease and metabolic syndrome. *Eur J Med Chem*. 2020;205:112649. https://doi.org/10.1016/j.ejmech.2020.112649.

26 Xie L, Yuan Y, Xu S, et al. Downregulation of hepatic ceruloplasmin ameliorates NAFLD *via* SCO1-AMPK-LKB1 complex. *Cell Rep*. 2022;41(3):111498. https://doi.org/10.1016/j.celrep.2022.111498.

27 Garcia D, Hellberg K, Chaix A, et al. Genetic liver-specific AMPK activation protects against diet-induced obesity and NAFLD. *Cell Rep*. 2019;26(1):192-208.e196. https://doi.org/10.1016/j.celrep.2018.12.036.

28 Poornima MS, Sindhu G, Billu A, et al. Pretreatment of hydroethanolic extract of *Dillenia indica* L. attenuates oleic acid induced NAFLD in HepG2 cells *via* modulating SIRT-1/p-LKB-1/AMPK, HMGCR & PPAR-α signaling pathways. *J Ethnopharmacol*. 2022;292:115237. https://doi.org/10.1016/j.jep.2022.115237.

29 Zhu X, Bian H, Wang L, et al. Berberine attenuates nonalcoholic hepatic steatosis through the AMPK-SREBP-1c-SCD1 pathway. *Free Radic Biol Med*. 2019;141:192-204. https://doi.org/10.1016/j.freeradbiomed.2019.06.019.

30 Hassan MA, Elmageed GMA, El-Qazaz IG, et al. The synergistic influence of polyflavonoids from *Citrus aurantifolia* on diabetes treatment and their modulation of the PI3K/AKT/FOXO1 signaling pathways: molecular docking analyses and *in vivo* investigations. *Pharmaceutics*. 2023;15(9):2306. https://doi.org/10.3390/pharmaceutics15092306.

31 Gao Y, Chu S, Zhang Z, et al. Hepataprotective effects of ginsenoside Rg1–a review. *J Ethnopharmacol*. 2017;206(16):178-183. https://doi.org/10.1016/j.jep.2017.04.012.

32 Luo J, Xu Q, Jiang B, et al. Selectivity, cell permeability and oral availability studies of novel bromophenol derivative HPN as protein tyrosine phosphatase 1B inhibitor. *Br J Pharmacol*. 2018;175(1):140-153. https://doi.org/10.1111/bph.14080.

33 Pang Y, Xu X, Xiang X, et al. High fat activates *O*-GlcNAcylation and affects AMPK/ACC pathway to regulate lipid metabolism. *Nutrients*. 2021;13(6):1740. https://doi.org/10.3390/nu13061740.

34 Fang K, Wu F, Chen G, et al. Diosgenin ameliorates palmitic acid-induced lipid accumulation *via* AMPK/ACC/CPT-1A and SREBP-1c/FAS signaling pathways in LO2 cells. *BMC Complement Altern Med*. 2019;19(1):255. https://doi.org/10.1186/s12906-019-2671-9.

35 Chen Y, He X, Chen X, et al. SeP is elevated in NAFLD and participates in NAFLD pathogenesis through AMPK/ACC pathway. *J Cell Physiol*. 2021;236(5):3800-3807. https://doi.org/10.1002/jcp.30121.

36 Mato JM, Alonso C, Noureddin M, et al. Biomarkers and subtypes of deranged lipid metabolism in non-alcoholic fatty liver disease. *World J Gastroenterol*. 2019;25(24):3009-3020. https://doi.org/10.3748/wjg.v25.i24.3009.

37 Xiao Z, Liu M, Yang F, et al. Programmed cell death and lipid metabolism of macrophages in NAFLD. *Front Immunol*. 2023;14:1118449. https://doi.org/10.3389/fimmu.2023.1118449.

38 Sfikas G, Psallas M, Koumaras C, et al. Prevalence, diagnosis, and treatment with 3 different statins of non-alcoholic fatty liver disease/non-alcoholic steatohepatitis in military personnel. Do genetics play a role? *Curr Vasc Pharmacol*. 2021;19(5):572-581. https://doi.org/10.2174/1570161118666201015152921.

39 Polyzos SA, Goulis DG, Giouleme O, et al. Anti-obesity medications for the management of nonalcoholic fatty liver disease. *Curr Obes Rep*. 2022;11(3):166-179. https://doi.org/10.1007/s13679-022-00474-0.

40 Filippatos TD, Derdemezis CS, Gazi IF, et al. Orlistat-associated adverse effects and drug interactions: a critical review. *Drug Saf*. 2008;31(1):53-65. https://doi.org/10.2165/00002018-200831010-00005.

41 Gerges SH, Wahdan SA, Elsherbiny DA, et al. Pharmacology of diosmin, a citrus flavone glycoside: an updated review. *Eur J Drug Metab Pharmacokinet*. 2022;47(1):1-18. https://doi.org/10.1007/s13318-021-00731-y.

42 Herzig S, Shaw RJ. AMPK: guardian of metabolism and mitochondrial homeostasis. *Nat Rev Mol Cell Biol*. 2018;19(2):121-135. https://doi.org/10.1038/nrm.2017.95.